Amygdalar and hippocampal volume loss in limbic-predominant age-related TDP-43 encephalopathy

Alex Wesseling,[1,2,3] Ismael L. Calandri,[2,3,4] Maud M. A. Bouwman,[1,2,4] Niels Reijner,[1,2,4] Natasja A. C. Deshayes,[1,2] Frederik Barkhof,[4,5,6] Rik Ossenkoppele,[2,3,4] Wilma D. J. van de Berg,[1,2,4] Annemieke E. Rozemuller,[7] Yolande A. L. Pijnenburg,[2,3] Jeroen J. M. Hoozemans[7,†] and Laura E. Jonkman[1,2,4]

Abstract

Limbic-predominant age-related TAR-DNA binding protein (TDP-43) encephalopathy neuropathological change (LATE-NC) refers to the aberrant accumulation of TDP-43 in the brains of aging individuals either in isolation or in combination with neurodegenerative disease. LATE-NC is most commonly found in the amygdala and hippocampus and is associated with progressive amnestic decline in individuals with a neurodegenerative disease. Since LATE-NC can only be diagnosed post-mortem, there is a need for pathology-validated neuroimaging biomarkers for LATE-NC. In the current study we assessed MRI-measured amygdalar and hippocampal volume in brain donors with Alzheimer's disease or Lewy Body diseases with and without co-occurring LATE-NC pathology.

Post-mortem *in-situ* 3D-T1 3T-MRI data were collected for 51 cases (27 Alzheimer's disease and 24 Lewy Body Disease) of whom 17 had post-mortem confirmed LATE-NC and 34 were non-LATE-NC (matched on age, sex, and neurodegenerative disease). Amygdalar and hippocampal volumes were calculated using FreeSurfer. Within-subject amygdalar and hippocampal tissue sections were immunostained for TDP-43 (pTDP-43), phosphorylated tau (AT8), amyloid-β (4G8) and α-synuclein (pSer129). Positive cell density (TDP-43 and α-synuclein) and area percentage immunoreactivity (p-tau and amyloid-β) outcome measures were quantified using QuPath. Group differences between LATE-NC and non-LATE-NC donors were assessed with univariate analyses and correlations were assessed with linear regression models, all adjusting for intracranial volume and post-mortem delay and if applicable for primary pathology.

Brain donors with LATE-NC showed significantly lower amygdalar (-26%, p=.014) and hippocampal (-19%, p=.003) volumes than non-LATE-NC brain donors, even when correcting for regional phosphorylated tau, amyloid-β and α-synuclein burden. These group differences remained significant in the Alzheimer's disease group (amygdala -24%, p=.028; hippocampus -21%, p=.002), but in the Lewy body diseases group only the amygdala was smaller in LATE-NC donors compared to non-LATE-NC donors (18%, p=.030). These results suggest that severity of TDP-43 burden plays a role in amygdala and hippocampus atrophy on MRI, even when correcting for effects of primary pathology. This study proposes that exceptionally low amygdalar and hippocampal volumes could indicate LATE-NC and that this may serve as a potential biomarker for *in-vivo* studies.

Author affiliations:

1 Department of Anatomy and Neurosciences, Amsterdam UMC, 1081 HV, Amsterdam, The Netherlands

2 Amsterdam Neuroscience, Neurodegeneration, 1081 HV Amsterdam, The Netherlands

3 Alzheimer Center Amsterdam UMC, 1081 HV Amsterdam, The Netherlands

4 Amsterdam Neuroscience, Brain Imaging, 1081 HV Amsterdam, The Netherlands

5 Department of Radiology and Nuclear Medicine, Amsterdam UMC, 1081 HV Amsterdam, The Netherlands

6 Queen Square Institute of Neurology and Centre for Medical Image Computing, University College London, Queen Square, London WC1N 3BG, UK

7 Department of Pathology, Amsterdam UMC, 1081 HV, Amsterdam, The Netherlands

†Present address: Roche Pharma Research and Early Development; Neuroscience and Rare Diseases Discovery and Translational Area, Roche Innovation Center, Basel, Switzerland

Correspondence to: Alex Wesseling

Department of Anatomy and neurosciences, de Boelelaan 1117, 1081 HV, Amsterdam, The Netherlands

E-maoil: a.j.wesseling@amsterdamumc.nl

Running title: Amygdalar and hippocampal volume in LATE-NC

Keywords: Alzheimer's disease; MRI; TDP-43; amygdala; neuropathology; Lewy body disease

Introduction

Limbic-predominant age-related TDP-43 encephalopathy neuropathological change (LATE-NC) is a recently proposed neuropathological entity that involves the aggregation of TDP-43 protein in the amygdala, hippocampus, and cortical regions.[1] Recent autopsy-based studies have found the prevalence of LATE-NC to be 20-55% in individuals older than 80 years.[2-4] In Alzheimer's disease (AD) patients, the prevalence of comorbid LATE-NC pathology has been reported to be between 20-60%,[1,5,6] with a lower prevalence of around 7-10% in early-onset AD (EOAD, age-at-onset <65 years).[7] Fewer studies have investigated the prevalence of LATE-NC pathology in Lewy body diseases (LBD), but LATE-NC seems to be more common in Parkinson's disease dementia (PDD; 19%) and dementia with Lewy bodies (DLB; 30-45%) compared to individuals with Parkinson's disease (PD) without dementia (7.2%).[8,9] The prevalence of LATE-NC in LBD might be higher in those with limbic- or amygdala-predominant LBD as opposed to neocortical-predominant LBD.[10]

LATE-NC is associated with impaired cognition in two ways: LATE is a clinical syndrome and a cause of cognitive decline independent of other neurodegenerative other neurodegenerative diseases[1,11] but LATE-NC pathology is also more prevalent in patients with neurodegenerative diseases.[12] In AD, those with LATE-NC pathology exhibit faster cognitive decline compared to AD patients without LATE-NC.[13,14]

Currently, there is no standardized neuroimaging-based assessment for LATE-NC during life, and it remains difficult to assess the extent to which LATE-NC pathology plays a role in the cognitive profile individuals during their lifetime. Several studies explored *in-vivo* magnetic

resonance imaging (MRI) with subsequent autopsy validation as a neuroimaging marker for LATE-NC in AD. They found more pronounced hippocampal atrophy in LATE-NC compared to non-LATE-NC AD donors.[15-18] More specifically, MRI volume and TDP-43 pathology were negatively associated in the anterior hippocampus[18] and cornu ammonis (CA) 1 region, indicating hippocampal (subfield) volume as a potential marker for LATE-NC.[15] Intervals of several years can limit the interpretation of post-mortem immunohistochemistry measures to *in-vivo* MRI data, because disease progression may obscure the role of LATE-NC pathology in the neurodegenerative process. Post-mortem MRI can overcome this challenge, as it has the unique advantage of allowing a direct comparison between imaging and pathology at the same moment in time. Several studies have used *ex-vivo* post-mortem imaging of formalin-fixed brain tissue to investigate neuropathological correlates of amygdalar and hippocampal atrophy,[19-21] and show that both p-tau and TDP-43 severity contribute to amygdalar and hippocampal volume loss.[18,21] Moreover they show that TDP-43 burden associates with amygdalar and hippocampal shape distortion,[19,21] suggesting that amygdalar and hippocampal subfields might be differently affected by LATE-NC pathology. Nevertheless, volumetric MRI studies performed on fixed brain tissue impair comparability to *in-vivo* MRI, as brain tissue can be distorted during the fixation process. Post-mortem *in-situ* (brain still in cranium) MRI could mitigate this limitation.[22]

The aim of the current study was to investigate the association between LATE-NC pathology and post-mortem *in-situ* MRI volume in a cohort of brain donors with AD and LBD. Furthermore, we aimed to investigate whether differences in amygdalar and hippocampal volume between LATE-NC and non-LATE-NC AD donors could already be identified on preceding *in-vivo* MRI. Lasty, we aimed to explore the relative contribution of TDP-43, p-tau, amyloid-β and α-synuclein pathology on post-mortem MRI volumes. Results of this study could provide insights towards amygdalar and hippocampal MRI volumes as neuroimaging biomarkers for LATE-NC.

Materials and methods

Donor inclusion

For an overview of our workflow, see figure 1. A total of 51 brain donors with clinically diagnosed and pathologically confirmed AD or LBD with available post-mortem *in-situ* MRI were included in this study. Of these, 45 donors were included in collaboration with the Netherlands Brain Bank (http://brainbank.nl), 6 donors were included in collaboration with the Normal Aging Brain Collection Amsterdam (www.nabca.eu). Neuropathological diagnosis was established by an expert neuropathologist (A.M.R.) according to the international guidelines of the BrainNet Europe II consortium (BNE).[23] Assessment of hippocampal sclerosis was performed on haematoxylin and eosin-stained hippocampal sections (see supplementary figure 1). Neuropathological assessment of LATE-NC pathology was done according to the guidelines by Nelson *et al.*[1] According to these guidelines, LATE-NC stage 1 includes TDP-43 positivity in either the amygdalar or (para)hippocampal regions, spreading to both regions in stage 2, and to the middle frontal gyrus in stage 3.[1,24]

Donors with a LATE-NC stage of 1, 2 or 3 (N=9 AD, N=8 LBD) were retrospectively selected from existing cohorts of donors with AD or LBD. A group of donors without LATE-NC pathology (N=18 AD, N=16 LBD) from the same cohorts was matched based on age, sex, and neuropathological staging within disease group (Braak neurofibrillary tangle (NFT) stage;[25] Thal phase;[26] and Braak Lewy Body stage[27]). If available, Clinical dementia rating (CDR) scores for all donors were obtained from the last clinical assessment or retrospectively by a general practitioner as a measure of cognitive decline. The donors had previously provided consent for the use of their brain tissue for research purposes.

MRI acquisition: in-situ and in-vivo

All donors underwent post-mortem 3T *in-situ* MRI according to a previously described pipeline.[28] Scans were acquired on a 3T scanner (Sigma-MRI750, General Electric Medical Systems, Milwaukee, WI) with an eight-channel phased-array head coil. T1-weighted images were

acquired using a sagittal 3D-T1-weighted fast spoiled gradient echo (GRE) sequence (repetition time (TR) = 7 ms; echo time (TE) = 3 ms; inversion time (TI) = 450 ms; flip angle = 15°; slice thickness = 1 mm; in-plane resolution = 1.0 x 1.0 mm^2). A sagittal 3D fluid attenuation inversion recovery (FLAIR) sequence was acquired with the following parameters: TR = 8000 ms; TE = 130 ms; TI = 2000-2250 ms; slice thickness = 1.2 mm; in-plane resolution = 1.11 x 1.11 mm^2. The inversion time of the post-mortem FLAIR sequence was optimized for each individual case to account for differences in CSF suppression due to body temperature.

Furthermore, 19 out of 24 Alzheimer's disease cases included in this study had ante-mortem *in-vivo* 3T MRI scans available, retrospectively included from the Amsterdam Dementia Cohort [29] using different scanners. For their T1-weighted images, the TR varied between 7.8 and 7.9 ms, and TE between 2.9 and 5.2 ms (see supplementary table 1) with voxel size fixed at 1 mm^3 isotropic. If more than one *in-vivo* MRI was available, the most recent one was used for our analysis. Time between most recent *in-vivo* MRI and death was between 4 days and 6 years with a mean of 3.3 years (SD 2.0 years).

MRI brain volume assessment

All post-mortem 3D-T1 images were lesion-filled based on the FLAIR images as previously described,[30] to reduce the effect of vascular burden on their tissue type segmentation. Parcellation of brain areas was performed with Freesurfer (Freesurfer), version 7.0,[31] using the Dekisan-Killaney atlas,[32] from which intracranial volume, amygdalar and hippocampal volumes from both hemispheres were extracted. Using the Freesurfer atlas by Saygin and colleagues,[33] the following amygdalar subfields were identified: lateral nucleus, basal nucleus, accessory basal nucleus, corticomedial nuclei (including the cortico-amygdaloid transition area, cortical and medial nuclei) and the central nucleus. Furthermore, the dentate gyrus, CA4 region, CA3 (including CA2) region, CA1 region, subiculum, and parasubiculum (including the presubiculum) were identified using the Hippocampal Subfield protocol with no head/body division (suffix FS60) for the hippocampus.[34] Additionally, visual MRI scores (Global cortical atrophy, parietal cortical atrophy, medial temporal lobe atrophy[42] and Fazekas score[40]) were determined by a clinical radiologist (F.B.)

Tissue sampling

Autopsy was performed directly after *in-situ* MRI acquisition, which resulted in a post-mortem delay of less than 13 hours for all subjects (mean post-mortem delay 7 hours and 35 minutes). Tissue blocks from the amygdala and hippocampus were collected from the right hemisphere after 4 weeks fixation. The hippocampal blocks were cut from the middle of the hippocampus to ensure inclusion of all subfields. The amygdalar blocks were cut to include the anterior part of the entorhinal cortex. All tissue blocks were subsequently paraffin embedded for immunohistochemistry.

Immunohistochemistry

Sections of 6µm were cut from the amygdalar and hippocampal blocks and mounted on superfrost+ glass slides (Thermo Fischer Scientific, Massachusetts, USA). Amygdalar and hippocampal tissue from all donors were stained for phosphorylated tau (p-tau, AT8, Thermo Fischer Scientific, Massachusetts, USA, 1:800 dilution), amyloid-β (4G8, Biolegend, California, USA 1:4000 dilution), phosphorylated α-synuclein (pSer-129, Abcam, United Kingdom 1:8000 dilution) and phosphorylated TDP-43 (pTDP-43, Cosmo Bio, Japan, 1:8000 dilution). All deparaffinized tissue sections were immersed in 10mM Citrate buffer (pH 6.0) for TDP-43, 4G8 and AT8 and in 10mM Tris-EDTA buffer (pH 9.0) for pSer-129 and heated to 120 ˚C in a steam cooker for antigen retrieval. Sections were blocked for 30 minutes for endogenous peroxidase (0.3%) in phosphorous buffer saline for TDP-43 (PBS; pH 7.4) and in tris buffered saline for pSer-129, 4G8 and AT8 (TBS; pH 7.4). Primary antibodies were diluted in PBS for TDP-43 and TBS for pSer-129, AT8 and 4G8 with 1% normal goat serum (ImmunoLogic, Duiven, The Netherlands) and 0.5% Triton and incubated overnight at 4 ˚C. Primary antibodies were detected using EnVision (Dako, Glostrup, Denmark) and visualised with 3.3'-Diaminobenzidine (DAB, Dako) with Imidazole (50 mg DAB, 350 mg Imidazole and 30 µL of H_2O_2 per 100mL of Tris-HCL 30 mM, pH 7.6). PBS (pTDP-43) or TBS (pSer-129; 4G8; AT8) was used in between steps to wash the sections. Finally, sections were counter-stained with haematoxylin, dehydrated, and mounted with Entellan (Merck, Darmstadt, Germany).

Image analysis

A whole-slide scanner (Olympus VS200; Evident; 20x objective) was used to visualise the sections which were subsequently quantified using QuPath version 3.2.0.[35] Hippocampal regions of interest were drawn to include the dentate gyrus, CA1-4, and (para)subiculum based on cytoarchitectural boundaries as previously described by Adler and colleagues.[36] The whole hippocampus was defined as the sum of these regions. The amygdala and its subnuclei were first segmented on a Nissl staining, after which the different subnuclei were identified and segmented on neuropathological stainings. The amygdala was segmented into the lateral, basal, accessory basal, central (including the central lateral and the central medial nuclei), and cortico-medial nuclei (including the peri-amygdaloid cortex, the cortical nuclei and the medial nuclei) according to Schumann and colleagues.[37]

For TDP-43 and α-synuclein, positive cells were counted using an object classifier, resulting in an outcome measure representing the Lewy Body/TDP-43 positive cell inclusion density in a region. For p-tau and amyloid-β, immunoreactivity of DAB staining was quantified using previously published pixel classifiers,[38,39] which resulted in an outcome measure representing area % immunoreactivity (see supplementary figure 2).

Statistics

Statistical analysis was performed using IBM SPSS 28.0 for Windows (SPSS, Inc., Chicago, USA) and R studio 4.4.3. All variables were tested for normality by visual inspection. MRI volume and p-tau load were normally distributed, but α-synuclein inclusion density, TDP-43 inclusion density, and amyloid-β load were not. These were transformed using log transformation, after which the transformed amyloid-β load and α-synuclein density were normally distributed. The log transformed TDP-43 positive cell count was still not normally distributed, and thus a Spearman rank test was used to investigate correlations with this variable. demographics between groups were compared using Mann-Whitney U test for continuous data and Fisher exact test for categorical data.

An ANCOVA was used to calculate group differences in MRI volume between LATE-NC and non-LATE-NC donors, both in the whole cohort as within AD and LBD separately. For analyses using *post-mortem* MRI volume data, post-mortem delay and intracranial volume were included as covariates, while for the *in-vivo* MRI analysis the intracranial volume and time between *in-vivo* and *post-mortem* MRI scans (in years) were controlled for. For analyses where primary pathology was corrected for, amyloid-β, p-tau and/or α-synuclein were included as covariates in the analysis. Since LATE-NC and non-LATE-NC donors were matched on sex and age and these variables did not differ between groups, these variables were not added as covariates in these analyses. Group differences in pathological load of p-tau, amyloid-β, α-synuclein and TDP-43 were calculated using t-tests to account for non-equal variance between groups. Analyses of the different amygdalar and hippocampal subfields were FDR corrected for multiple comparisons. For the estimation of the ROC curve, R version 4.4.1 (2024-06-14 ucrt) and the pROC[54] package were used.

Correlations between amyloid-β, α-synuclein and p-tau were investigated using Pearson correlations, while correlations between TDP-43 and amyloid-β, α-synuclein or p-tau were assessed using Spearman rank tests. Correlations between pathologies were only performed in donors with pathology in this region. For the amygdala this was defined as LATE-NC ≥1, Braak LB ≥4, Braak NFT ≥4, and Thal ≥ 3. For the hippocampus this was defined as LATE-NC ≥2, Braak LB ≥3, Braak NFT ≥1, and Thal ≥2. Correlations between different pathological measures were FDR-corrected for multiple comparisons.

To investigate the combined effect of TDP-43, p-tau, α-synuclein and amyloid-β on amygdalar and hippocampal volume, and to identify which pathological hallmark(s) was/were the strongest driver(s) of MRI volume loss, linear regression analysis with backward selection was performed. This model included MRI volume as dependent variable and included the four pathological markers in a backward model as well as intracranial volume as a separate variable.

Results

Donor characteristics

Demographic, clinical, radiological, and pathological data from donors are summarized in table 1. Clinical diagnosis, age at death, sex and Fazekas score[40] did not differ between LATE-NC and non-LATE-NC groups, whereas LATE-NC donors had a shorter average disease duration (p=.047), as well as a higher CDR scores[41] (p=.020), and medial temporal lobe atrophy (MTA)[42] scores (p=.014). LATE-NC donors did not differ in post-mortem delay (PMD), *APOE4* genotype, presence of atherosclerosis, Thal phase[26],Braak Lewy Body[27] or Braak NFT[25] stage from non-LATE-NC donors. LATE-NC donors also had higher incidence of hippocampal sclerosis (p=.001). For a summary of individual data, see supplementary table 2.

LATE-NC donors have lower amygdalar and hippocampal MRI volumes

Without correction for primary pathology, brain donors with LATE-NC had a 22% lower right hemisphere (ipsilateral to pathological data) amygdalar (p=.001) and 13% lower hippocampal (p=.009) volume compared to non-LATE-NC donors. Furthermore, a significant reduction of 15% in amygdalar (p=.035) but not hippocampal volume (p=.842) was found in the left hemisphere. When correcting for p-tau, amyloid-β, and α-synuclein, the difference in volume between LATE-NC and non-LATE-NC donors increased for the amygdala (26% volume reduction, p=.014) and hippocampus (19% volume reduction, p=.003) of the right hemisphere (figure 2a), but was not significant for the amygdala and hippocampus of the left hemisphere.

Within the right hemisphere, when investigating different amygdala subnuclei, only the lateral nucleus (-20%, p=.014) was significantly smaller in LATE-NC donors compared to non-LATE-NC donors (figure 3a). In the hippocampus, the dentate gyrus (-20%, p=.002), CA1 (-20%, p=.027), CA2-3 (-24%, p=.002) and CA4 (-22%, p=.002) were significantly smaller in LATE-NC compared to non-LATE-NC donors (figure 3b).

To investigate whether MRI-measured amygdala and hippocampal volume are valuable predictors of LATE-NC we created a ROC curve to visualise the area under the curve (AUC) for MTA score, amygdalar and hippocampal volume (corrected for ICV). The AUC of amygdalar (.777) and hippocampal (.715) volume was similar compared to that of MTA score (.715) (figure 4).

MRI atrophy patterns differ between LATE-NC AD and LATE-NC LBD donors

When investigating LATE-NC AD and LBD donors separately, LATE-NC AD donors showed a similar pattern with smaller amygdalar (-26%, p=.009) and hippocampal (-17%, p=.007) volumes in the right hemisphere but not in the left hemisphere (amygdala: p=.146; hippocampus: p=.457) compared to non-LATE-NC AD donors. These group differences remained when controlling for p-tau and amyloid-β (amygdala: 24%, p=.028; hippocampus: 21%, p=.002) (figure 2b). LATE-NC LBD donors only had smaller amygdalar volumes (-19%, p=.045) but no hippocampal (p=.336) or left hemisphere (amygdala: p=.158; hippocampus: p=.715) volume difference compared to non-LATE-NC LBD donors. These results remained the same when controlling for α-synuclein (amygdala: -18%, p=.030; hippocampus: p=.277) (figure 2c).

Post-mortem hippocampal volume reflects in-vivo volume

In-vivo MRI was available for five LATE-NC and twelve non-LATE-NC donors. When comparing *in-vivo* MRI volumes between LATE-NC and non-LATE-NC AD donors, we found that hippocampal (18%, p=.007), but not amygdalar (p=.083) volumes were significantly lower in LATE-NC donors (figure 5a). Figure 5b shows the correlation between *in-vivo* and post-mortem MRI volume, corrected for time between the two MRI scans (r=.97; p=.001).

Neuropathological burden in LATE-NC and non-LATE-NC

By definition, LATE-NC donors had significantly higher TDP-43 positive cell density in the amygdala (p=.023) and hippocampus (p=.004) compared to non-LATE-NC donors (figure 6a-b). When investigating different amygdalar and hippocampal subregions, we found significantly higher TDP-43 pathology in all amygdala subnuclei, as well as in the CA1, CA4, subiculum and parasubiculum of the hippocampus. LATE-NC AD donors did not differ from non-LATE-NC AD donors on pathological load of p-tau, amyloid-β or α-synuclein density. However, LATE-NC LBD donors had significantly higher amyloid-β (p=.041) and p-tau load (p=.020) in the hippocampus compared to non-LATE-NC LBD donors (figure 6c, e). More specifically, LATE-NC LBD donors had higher p-tau load in all individual hippocampal subfields (figure 6f). None of the hippocampal subregions showed significantly higher amyloid-β load in LATE-NC LBD donors compared to non-LATE-NC LBD donors (figure 6d).

For a detailed overview of observed correlations between pathologies, please refer to supplementary table 3. P-tau and amyloid-β load were positively correlated in the whole hippocampus (r=.51; p=.003*)* and all subfields separately, as well as in the accessory basal nucleus of the amygdala (r=.54; p=.030). No significant correlations between other pathologies including TDP-43 were reported after FDR-correcting for multiple comparisons.

TDP-43 predicts amygdalar volume in LATE-NC donors

To explore which pathological aggregate(s) (TDP-43, p-tau, α-syn and amyloid-β), best explained variance in amygdalar and hippocampal volume, we conducted an exploratory analysis using a linear regression model in our entire cohort. The final model predicting amygdalar volume included TDP-43 (β=-.24, p=.091), p-tau (β=-.33, p=.020) and intracranial volume (β=.45, p=.001) and had a total adjusted R^2 of .401. The final model predicting hippocampal volume included TDP-43 (β=-.38, p=.002), p-tau (β=-.26, p=.030) and intracranial volume (β=.42, p=.001) and had a total adjusted R^2 of .515. Supplementary figure 4 shows the volume of donors with different combinations of neuropathologies.

We also performed the same prediction model as above in the LATE-NC group only. Among the four pathological aggregates, TDP-43 was the strongest predictor of amygdalar volume within LATE-NC donors. The final model included TDP-43 (β=-.67, p=.013) and intracranial volume (β=.98, p=.002) as significant predictors and had a total adjusted R^2 of .631. The model that best predicted hippocampal volume included only intracranial volume (β=.78, p=.002) and none of the pathological aggregates.

Discussion

Using a post-mortem *in-situ* MRI and concurrent immunohistochemistry approach, we found that LATE-NC donors had lower amygdalar and hippocampal volumes compared to non-LATE-NC donors, even when accounting for the contribution of primary amyloid-β, p-tau and α-syn pathologies. Furthermore, we found that TDP-43 cell density predicted volume loss in the amygdala of LATE-NC donors. These findings suggest that TDP-43 pathology in LATE-NC plays a role in amygdalar volume loss, independently of primary pathology.

In line with earlier literature,[5] LATE-NC donors had higher CDR scores compared to non-LATE-NC donors, indicative of more cognitive impairment. This finding, in combination with the shorter disease duration in LATE-NC compared to non-LATE-NC donors, suggests that donors with LATE-NC have a faster cognitive decline. Early clinical recognition of LATE-NC co-pathology is therefore important for an accurate clinical prognosis. Interestingly, 2 out of 17 LATE-NC donors had a disease onset before the age of 65, which suggests that it is important to consider LATE-NC not just as a pathology in older individuals.[1,43]

In LATE-NC donors, our study found a decrease in post-mortem amygdalar volume between 22% and 26% as well as a decrease between 15% and 19% for hippocampal volume, depending on hemisphere and disease group. This is in line with Bejanin and colleagues (2019) reporting between 5 and 15% *in-vivo* amygdalar and hippocampal volume loss in neuropathological confirmed LATE-NC compared to non-LATE-NC individuals.[16] Several other studies reporting amygdalar and/or hippocampal volume loss in LATE-NC donors, do not specify the exact difference in MRI volumes.[17,19] Interestingly, the volume loss in LATE-NC compared to non-LATE-NC donors was greater (26% amygdala and 20% hippocampus) after controlling for primary

pathology, suggesting that the amount of atrophy that can be contributed to LATE-NC pathology might be greater than previously thought.

Lower volumes of the medial temporal lobe in LATE-NC donors were also reflected by lower post mortem MTA scores[42] in LATE-NC donors compared to non-LATE-NC donors. Furthermore, MTA seemed to be equal to hippocampal and amygdalar volume in distinguishing LATE-NC from non-LATE-NC. The MTA score has previously been reported to be a sensitive marker for hippocampal atrophy in AD[51], but according to our study it might also be a valuable tool for recognizing LATE, not just in AD but also in LBD patients. This is in line with a recent paper by Wolk and colleagues (2025)[52] who suggest that including MTA scores could be valuable in defining possible and probable LATE.

In addition to lower right hemisphere amygdalar and hippocampal volumes, we found lower left hemisphere amygdalar volumes in LATE-NC compared to non-LATE-NC donors. However, we found no difference in left hippocampal volumes. These findings can be explained by a possible asymmetry in LATE-NC pathology[44,45] or the fact that our LATE-NC diagnosis was established on tissue from the right hemisphere. In future endeavours it would be worthwhile to sample the amygdala and hippocampus bilaterally.

Our results show that LATE-NC AD donors had lower amygdalar and hippocampal volumes compared to non-LATE-NC AD donors, but LATE-NC LBD donors only had lower amygdalar volumes compared to non-LATE-NC LBD donors, while we found no difference in hippocampal volume between LATE-NC and non-LATE-NC LBD donors. This could mean within LBD patients, amygdalar volume might be a better indicator of LATE-NC compared to hippocampal volume.

When investigating volumetric differences in amygdalar subnuclei of LATE-NC compared to non-LATE-NC donors, we found that specifically the lateral nucleus was smaller in LATE-NC compared to non-LATE-NC donors. This is partially in line with findings from Makkinejad and colleagues,[21] who describe a negative association of TDP-43 and basolateral and superficial nuclei on *ex-vivo* MRI volume in LATE-NC donors. The lateral nucleus of the amygdala contains the most connecting fibres to the hippocampus and entorhinal cortex,[46,47] possibly explaining faster cognitive decline compared to non-LATE-NC donors and explaining the spread of TDP-43 to the hippocampus.

In the hippocampus we found lower dentate gyrus and CA1-4 volumes in LATE-NC donors compared to non-LATE-NC donors. We did not find a significant volumetric difference for the subiculum, even though this region had the highest TDP-43 inclusion load. This is in line with an *ex-vivo* MRI study by Wisse and colleagues (2021)[19], but not with a study by Hanko and colleagues (2019).[19] Furthermore, one study by de Flores and colleagues (2020) reported a selective TDP-43-associated volume loss in the anterior hippocampus.[18] Since we only investigated the middle part of the hippocampus, we are unable to replicate this finding.

Using the available *in-vivo* MRI data from our AD cohort, we found that LATE-NC donors showed lower hippocampal volumes compared to non-LATE-NC donors. This is in line with other studies[18,16] and suggests that lower hippocampal volume can play a role in distinguishing AD from LATE-NC AD in a clinical setting, for example by investigating the rate of hippocampal compared to global atrophy. Unlike the Bejanin *et al*[16] study, we did not find a significant difference between LATE-NC AD and non-LATE-NC AD amygdalar volumes. One explanation for this discrepancy could be the low statistical power due to a limited number of available *in-vivo* MRIs (*N*=5) of LATE-NC AD donors. Furthermore, *in-vivo* volume loss in the hippocampus might be amplified by co-occuring hippocampal sclerosis.

The distribution of TDP-43 inclusions in the amygdala is relatively uniform across subnuclei, but in the hippocampus we report the highest inclusion density in the subiculum and CA1. Little is known about relative TDP-43 burden in amygdalar subnuclei, but TDP-43 burden in the subiculum, CA1 and dentate gyrus in LATE-NC has been reported in several studies.[12,48,49] Interestingly, Uemura *et al*[12] report differences in distribution of TDP-43 between LATE-NC AD and LATE-NC LBD in the hippocampus, including a relative increase in TDP-43 burden in the CA2 and CA3 in LATE-NC LBD.[12] Although we find similar findings (see supplementary figure 3), this increase in CA2-3 density is mainly driven by two cases. We report higher amyloid-β and p-tau load in LATE-NC LBD compared to non-LATE-NC LBD donors, which is in line with earlier studies that report higher AD co-pathology in LATE-NC LBD compared to non-LATE-NC LBD individuals.[12,50] Several studies also found increased Lewy body pathology in LATE-NC AD donors compared to non-LATE-NC AD donors,[2,5] however we do not replicate this finding. Nevertheless, in our post-mortem MRI study, our neuropathological findings are based on a single section of the amygdala and hippocampus. Sampling throughout these regions in a larger cohort is

recommended to provide a more comprehensive overview of the association between TDP-43 and other pathologies in AD and LBD.

When investigating associations between post-mortem MRI and TDP-43 density in LATE-NC donors, we found that TDP-43 burden predicted amygdalar volume, in line with earlier research.[21] However we did not find any significant association between TDP-43 burden and volume in the hippocampus. As previously mentioned, this could be due to TDP-43-associated volume differences seen mostly within the anterior hippocampus,[18] but also the generally lower hippocampal TDP-43 inclusion density compared to the amygdala. The hippocampus most often is affected at a later LATE-NC stage compared to the amygdala.[24] Furthermore, measured TDP-43 burden at end stage of the disease might not necessarily reflect LATE-NC severity because severe neuronal loss might lead to reduction of TDP-43 neuronal inclusions.

The main strength of this study is the use of post-mortem *in-situ* MRI combined with pathological data of donors with clinically diagnosed and pathological confirmed neurodegenerative disease. However, there are also several limitations to this study. First, due to our relatively small sample size we were unable to investigate differences in association between TDP-43 and volume in AD and LBD separately. Small sample size also affected the power of our *in-vivo* MRI analyses. It should also be mentioned that subfield segmentations on 3T T1-weighted MRI have limited accuracy as they are only an approximation of the true subfields.[53] Lastly, the pathological data was retrospectively obtained from only the right hemisphere. Since LATE-NC can affect both hemispheres at different stages and severity levels,[44,45] investigating only one hemisphere provides only part of the picture of LATE-NC and its associated volume loss. In conclusion, more research needs to be done on individuals with LATE without neurodegenerative disease and how to distinguish cognitive decline due to LATE from cognitive decline due to AD or types of dementia.

Taken together, our study suggests that TDP-43 pathology in the context of LATE-NC is associated with a 26% lower amygdalar, and a 19% lower hippocampal volume in donors with end-stage neurodegenerative disease. TDP-43 burden appears to be an important predictor of amygdalar and hippocampal atrophy, the effects of which can already be observed *in-vivo*. Since LATE is associated with a faster disease course and worse cognitive outcomes, these results are relevant

towards the development of amygdalar and hippocampal volumes as potential biomarkers for possible LATE in a clinical setting.

Data availability

Data from the current study are available upon reasonable request.

Acknowledgements

We would like to thank the donors and their families for their valuable contribution. We would also like to thank the Netherlands Brain Bank (www.brainbank.nl) and Normal Aging Brain Collection Amsterdam (http://www.nabca.eu/) autopsy teams.

Funding

A.J.W and Y.A.L.P. are recipients of YOD-MOLECULAR, receiving funding from NWO (#KICH1.GZ02.20.004) as part of the NWO Research Program KIC 2020-2023 MISSION - Living with dementia. YOD-MOLECULAR receives co-financing from Winterlight Labs, ALLEO Labs (as part of Immuneering), and Hersenstichting. Team Alzheimer also contributes to YOD-MOLECULAR. R.O. has received research funding/support from European Research Council, ZonMw, NWO, National Institute of Health, Alzheimer Association, Alzheimer Nederland, Stichting Dioraphte, Cure Alzheimer's fund, Health Holland, ERA PerMed, Alzheimerfonden and Hjarnfonden. L.E.J receives active funding from the Alzheimer Association (AARG-22-974381), The Dutch Top Sector Life Sciences and Health (S-000438), The Netherlands Organization for Health Research and Development (09120012110015). F.B. is supported by the NIHR biomedical research centre at the UCLH. F.B. is also the Steering committee or Data Safety Monitoring Board member for Biogen, Merck, Eisai and Prothena. Advisory board member for Combinostics, Scottish Brain Sciences, Alzheimer Europe. Consultant for Roche, Celltrion, Rewind Therapeutics, Merck, Bracco. Research agreements with ADDI, Merck, Biogen, GE Healthcare, Roche. Co-founder and shareholder of Queen Square Analytics LTD. W.V.D.B. was financially supported by grants from Dutch Research council (ZonMW 70-73305-98-106; 70-73305-98-102; 40-46000-98-

101), Alzheimer association (AARF-18-566459), The Michael J. Fox foundation (MJFF-009210; MJFF-022468), Parkinson Association (2020-G01), Stichting Woelse Waard, Health Holland and Horizon Europe (NEUROCOV), Hoffmann-La Roche and Genentech. W.V.D.B. performed contract research for Roche Tissue Diagnostics, Discoveric Bio, AC Immune and received research consumables from Hoffmann-La Roche and Prothena.

Competing interests

R.O. has received research funding/support from Avid Radiopharmaceuticals, Janssen Research & Development, Roche, Quanterix and Optina Diagnostics, has given lectures in symposia sponsored by GE Healthcare, is an advisory board member for Asceneuron and a steering committee member for Biogen and Bristol Myers Squibb. J.J.M.H. is employed by F. Hoffmann-La Roche.L.E.J. has received research support (to the institution) from Imeka for unrelated work. W.V.D.B. is a member of the scientific advisory board of Alzheimer Nederland and Gain Therapeutics. She is the president of the association of Dutch Parkinson scientist and board member of the Parkinsonalliance Netherlands.

Supplementary material

Supplementary material is available at *Brain* online.

References

1. Nelson PT, Dickson DW, Trojanowski JQ, et al. Limbic-predominant age-related TDP-43 encephalopathy (LATE): consensus working group report. *Brain*. Jun 1 2019;142(6):1503-1527. doi:10.1093/brain/awz099

2. Agrawal S, Yu L, Kapasi A, et al. Limbic-predominant age-related TDP-43 encephalopathy neuropathologic change and microvascular pathologies in community-dwelling older persons. *Brain Pathol.* May 2021;31(3):e12939. doi:10.1111/bpa.12939

3. Nag S, Yu L, Wilson RS, Chen EY, Bennett DA, Schneider JA. TDP-43 pathology and memory impairment in elders without pathologic diagnoses of AD or FTLD. *Neurology*. Feb 14 2017;88(7):653-660. doi:10.1212/WNL.0000000000003610

4. Nelson PT, Fardo DW, Wu X, Aung KZ, Cykowski MD, Katsumata Y. Limbic-predominant age-related TDP-43 encephalopathy (LATE-NC): Co-pathologies and genetic risk factors provide clues about pathogenesis. *J Neuropathol Exp Neurol*. Apr 13 2024;doi:10.1093/jnen/nlae032

5. Josephs KA, Whitwell JL, Weigand SD, et al. TDP-43 is a key player in the clinical features associated with Alzheimer's disease. *Acta Neuropathol*. 2014;127(6):811-24. doi:10.1007/s00401-014-1269-z

6. Amador-Ortiz C, Lin WL, Ahmed Z, et al. TDP-43 immunoreactivity in hippocampal sclerosis and Alzheimer's disease. *Ann Neurol*. May 2007;61(5):435-45. doi:10.1002/ana.21154

7. Davidson YS, Raby S, Foulds PG, et al. TDP-43 pathological changes in early onset familial and sporadic Alzheimer's disease, late onset Alzheimer's disease and Down's syndrome: association with age, hippocampal sclerosis and clinical phenotype. *Acta Neuropathol*. Dec 2011;122(6):703-13. doi:10.1007/s00401-011-0879-y

8. Nakashima-Yasuda H, Uryu K, Robinson J, et al. Co-morbidity of TDP-43 proteinopathy in Lewy body related diseases. *Acta Neuropathol*. Sep 2007;114(3):221-9. doi:10.1007/s00401-007-0261-2

9. Higashi S, Iseki E, Yamamoto R, et al. Concurrence of TDP-43, tau and alpha-synuclein pathology in brains of Alzheimer's disease and dementia with Lewy bodies. *Brain Res*. Dec 12 2007;1184:284-94. doi:10.1016/j.brainres.2007.09.048

10. Besser LM, Teylan MA, Nelson PT. Limbic Predominant Age-Related TDP-43 Encephalopathy (LATE): Clinical and Neuropathological Associations. *J Neuropathol Exp Neurol*. Mar 1 2020;79(3):305-313. doi:10.1093/jnen/nlz126

11. Harrison WT, Lusk JB, Liu B, et al. Limbic-predominant age-related TDP-43 encephalopathy neuropathological change (LATE-NC) is independently associated with dementia and strongly associated with arteriolosclerosis in the oldest-old. *Acta Neuropathol*. Nov 2021;142(5):917-919. doi:10.1007/s00401-021-02360-w

12. Uemura MT, Robinson JL, Cousins KAQ, et al. Distinct characteristics of limbic-predominant age-related TDP-43 encephalopathy in Lewy body disease. *Acta Neuropathol*. Jan 2022;143(1):15-31. doi:10.1007/s00401-021-02383-3

13. Thomas DX, Bajaj S, McRae-McKee K, Hadjichrysanthou C, Anderson RM, Collinge J. Association of TDP-43 proteinopathy, cerebral amyloid angiopathy, and Lewy bodies with cognitive impairment in individuals with or without Alzheimer's disease neuropathology. *Sci Rep*. Sep 3 2020;10(1):14579. doi:10.1038/s41598-020-71305-2

14. Kapasi A, Yu L, Boyle PA, Barnes LL, Bennett DA, Schneider JA. Limbic-predominant age-related TDP-43 encephalopathy, ADNC pathology, and cognitive decline in aging. *Neurology*. Oct 6 2020;95(14):e1951-e1962. doi:10.1212/WNL.0000000000010454

15. Hanko V, Apple AC, Alpert KI, et al. In vivo hippocampal subfield shape related to TDP-43, amyloid beta, and tau pathologies. *Neurobiol Aging*. Feb 2019;74:171-181. doi:10.1016/j.neurobiolaging.2018.10.013

16. Bejanin A, Murray ME, Martin P, et al. Antemortem volume loss mirrors TDP-43 staging in older adults with non-frontotemporal lobar degeneration. *Brain*. Nov 1 2019;142(11):3621-3635. doi:10.1093/brain/awz277

17. Josephs KA, Dickson DW, Tosakulwong N, et al. Rates of hippocampal atrophy and presence of post-mortem TDP-43 in patients with Alzheimer's disease: a longitudinal retrospective study. *Lancet Neurol*. Nov 2017;16(11):917-924. doi:10.1016/S1474-4422(17)30284-3

18. de Flores R, Wisse LEM, Das SR, et al. Contribution of mixed pathology to medial temporal lobe atrophy in Alzheimer's disease. *Alzheimers Dement*. Jun 2020;16(6):843-852. doi:10.1002/alz.12079

19. Wisse LEM, Ravikumar S, Ittyerah R, et al. Downstream effects of polypathology on neurodegeneration of medial temporal lobe subregions. *Acta Neuropathol Commun*. Jul 21 2021;9(1):128. doi:10.1186/s40478-021-01225-3

20. Ravikumar S, Wisse LEM, Lim S, et al. Ex vivo MRI atlas of the human medial temporal lobe: characterizing neurodegeneration due to tau pathology. *Acta Neuropathol Commun*. Oct 24 2021;9(1):173. doi:10.1186/s40478-021-01275-7

21. Makkinejad N, Schneider JA, Yu J, et al. Associations of amygdala volume and shape with transactive response DNA-binding protein 43 (TDP-43) pathology in a community cohort of older adults. *Neurobiol Aging*. May 2019;77:104-111. doi:10.1016/j.neurobiolaging.2019.01.022

22. Boon BDC, Pouwels PJW, Jonkman LE, et al. Can post-mortem MRI be used as a proxy for in vivo? A case study. *Brain Commun*. 2019;1(1):fcz030. doi:10.1093/braincomms/fcz030

23. Klioueva NM, Rademaker MC, Dexter DT, et al. BrainNet Europe's Code of Conduct for brain banking. *J Neural Transm (Vienna)*. Jul 2015;122(7):937-40. doi:10.1007/s00702-014-1353-5

24. Nelson PT, Lee EB, Cykowski MD, et al. LATE-NC staging in routine neuropathologic diagnosis: an update. *Acta Neuropathology*. 2022;doi:https://doi.org/10.1007/s00401-022-02524-2

25. Braak H, Braak E. Neuropathological stageing of Alzheimer-related changes. *Acta Neuropathology*. 1991;82:239-259.

26. Thal DR, Rüb U, Orantes M, Braak H. Phases of Aβ-deposition in the human brain and its relevance for the development of AD. *Neurology*. 2002;58:1791-1800.

27. Braak H, Tredici KD, Rüb U, Vos RAId, Steur ENHJ, Braak E. Staging of brain pathology related to sporadic Parkinson's disease. *Neurobiology of aging*. 2003;24:197-211.

28. Jonkman LE, Graaf YG, Bulk M, et al. Normal Aging Brain Collection Amsterdam (NABCA): A comprehensive collection of postmortem high-field imaging, neuropathological and morphometric datasets of non-neurological controls. *Neuroimage Clin*. 2019;22:101698. doi:10.1016/j.nicl.2019.101698

29. van der Flier WM, Scheltens P. Amsterdam Dementia Cohort: Performing Research to Optimize Care. *J Alzheimers Dis*. 2018;62(3):1091-1111. doi:10.3233/JAD-170850

30. Steenwijk MD, Pouwels PJ, Daams M, et al. Accurate white matter lesion segmentation by k nearest neighbor classification with tissue type priors (kNN-TTPs). *Neuroimage Clin*. 2013;3:462-9. doi:10.1016/j.nicl.2013.10.003

31. Dale AM, Fischl B, Sereno MI. Cortical surface-based analysis. I. Segmentation and surface reconstruction. *Neuroimage*. Feb 1999;9(2):179-94. doi:10.1006/nimg.1998.0395

32. Desikan RS, Segonne F, Fischl B, et al. An automated labeling system for subdividing the human cerebral cortex on MRI scans into gyral based regions of interest. *Neuroimage*. Jul 1 2006;31(3):968-80. doi:10.1016/j.neuroimage.2006.01.021

33. Saygin ZM, Kliemann D, Iglesias JE, et al. High-resolution magnetic resonance imaging reveals nuclei of the human amygdala: manual segmentation to automatic atlas. *Neuroimage*. Jul 15 2017;155:370-382. doi:10.1016/j.neuroimage.2017.04.046

34. Iglesias JE, Augustinack JC, Nguyen K, et al. A computational atlas of the hippocampal formation using ex vivo, ultra-high resolution MRI: Application to adaptive segmentation of in vivo MRI. *Neuroimage*. Jul 15 2015;115:117-37. doi:10.1016/j.neuroimage.2015.04.042

35. Bankhead P, Loughrey MB, Fernandez JA, et al. QuPath: Open source software for digital pathology image analysis. *Sci Rep*. Dec 4 2017;7(1):16878. doi:10.1038/s41598-017-17204-5

36. Adler DH, Pluta J, Kadivar S, et al. Histology-derived volumetric annotation of the human hippocampal subfields in postmortem MRI. *Neuroimage*. Jan 1 2014;84:505-23. doi:10.1016/j.neuroimage.2013.08.067

37. Schumann CM, Bauman MD, Amaral DG. Abnormal structure or function of the amygdala is a common component of neurodevelopmental disorders. *Neuropsychologia*. Mar 2011;49(4):745-59. doi:10.1016/j.neuropsychologia.2010.09.028

38. Frigerio I, Boon BDC, Lin CP, et al. Amyloid-beta, p-tau and reactive microglia are pathological correlates of MRI cortical atrophy in Alzheimer's disease. *Brain Commun*. 2021;3(4):fcab281. doi:10.1093/braincomms/fcab281

39. Frigerio I, Laansma MA, Lin CP, et al. Neurofilament light chain is increased in the parahippocampal cortex and associates with pathological hallmarks in Parkinson's disease dementia. *Transl Neurodegener*. Jan 20 2023;12(1):3. doi:10.1186/s40035-022-00328-8

40. Fazekas F, Chawluk JB, Alavi A, Hurtig HI, Zimmerman RA. MR signal abnormalities at 1.5 T in Alzheimer's dementia and normal aging. *AJR Am J Roentgenol*. Aug 1987;149(2):351-6. doi:10.2214/ajr.149.2.351

41. Hughes CP, Berg L, Danziger WL, Coben LA, Martin RL. A new clinical scale for the staging of dementia. *Br J Psychiatry*. Jun 1982;140:566-72. doi:10.1192/bjp.140.6.566

42. Scheltens P, Leys D, Barkhof F, et al. Atrophy of medial temporal lobes on MRI in "probable" Alzheimer's disease and normal ageing: diagnostic value and neuropsychological correlates. *J Neurol Neurosurg Psychiatry*. Oct 1992;55(10):967-72. doi:10.1136/jnnp.55.10.967

43. Brenowitz WD, Monsell SE, Schmitt FA, Kukull WA, Nelson PT. Hippocampal sclerosis of aging is a key Alzheimer's disease mimic: clinical-pathologic correlations and comparisons with both alzheimer's disease and non-tauopathic frontotemporal lobar degeneration. *J Alzheimers Dis*. 2014;39(3):691-702. doi:10.3233/JAD-131880

44. King A, Bodi I, Nolan M, Troakes C, Al-Sarraj S. Assessment of the degree of asymmetry of pathological features in neurodegenerative diseases. What is the significance for brain banks? *J Neural Transm (Vienna)*. Oct 2015;122(10):1499-508. doi:10.1007/s00702-015-1410-8

45. Stefanits H, Budka H, Kovacs GG. Asymmetry of neurodegenerative disease-related pathologies: a cautionary note. *Acta Neuropathol*. Mar 2012;123(3):449-52. doi:10.1007/s00401-011-0936-6

46. Pikkarainen M, Ronkko S, Savander V, Insausti R, Pitkanen A. Projections from the lateral, basal, and accessory basal nuclei of the amygdala to the hippocampal formation in rat. *J Comp Neurol*. Jan 11 1999;403(2):229-60.

47. Pitkanen A, Kelly JL, Amaral DG. Projections from the lateral, basal, and accessory basal nuclei of the amygdala to the entorhinal cortex in the macaque monkey. *Hippocampus*. 2002;12(2):186-205. doi:10.1002/hipo.1099

48. Buciuc M, Whitwell JL, Baker MC, Rademakers R, Dickson DW, Josephs KA. Old age genetically confirmed frontotemporal lobar degeneration with TDP-43 has limbic predominant TDP-43 deposition. *Neuropathol Appl Neurobiol*. Dec 2021;47(7):1050-1059. doi:10.1111/nan.12727

49. Josephs KA, Murray ME, Whitwell JL, et al. Updated TDP-43 in Alzheimer's disease staging scheme. *Acta Neuropathol*. Apr 2016;131(4):571-85. doi:10.1007/s00401-016-1537-1

50. McAleese KE, Walker L, Erskine D, Thomas AJ, McKeith IG, Attems J. TDP-43 pathology in Alzheimer's disease, dementia with Lewy bodies and ageing. *Brain Pathol*. Jul 2017;27(4):472-479. doi:10.1111/bpa.12424

51. Barkhof F, Polvikoski TM, van Straaten EC, et al. The significance of medial temporal lobe atrophy: a postmortem MRI study in the very old. Neurology. Oct 9 2007;69(15):1521-7. doi:10.1212/01.wnl.0000277459.83543.99

52. Wolk DA, Nelson PT, Apostolova L, et al. Clinical criteria for limbic-predominant age-related TDP-43 encephalopathy. Alzheimers Dement. Jan 2025;21(1):e14202. doi:10.1002/alz.14202

53. Wisse LEM, Chételat G, Daugherty AM, et al. Hippocampal subfield volumetry from structural isotropic 1 mm^3 MRI scans: A note of caution. *Hum Brain Mapp*. 2021;42(2):539-550. doi:10.1002/hbm.25234

54. Robin, X., Turck, N., Hainard, A. *et al.* pROC: an open-source package for R and S+ to analyze and compare ROC curves. *BMC Bioinformatics* **12**, 77 (2011). https://doi.org/10.1186/1471-2105-12-77

Figure legends

Figure 1 Post-mortem MRI-pathology pipeline. For 51 donors, post-mortem 3T in-situ MRI was obtained, and amygdala and hippocampal subfield volumes were calculated with FreeSurfer[33,34] from the 3D-T1 image (yellow box). Autopsy was performed after MRI acquisition, and amygdala and hippocampal tissue was processed for immunohistochemistry against TDP-43, Aβ, p-tau, and α-syn (green and blue boxes). Regions of interest were drawn for the hippocampal subfields[36] and amygdala subnuclei,[37] to include the same regions as segmented on MRI (green box). Final quantitative outcome measures were obtained using object and pixelclassifiers in Qupath (blue box).[35] AD = Alzheimer's disease; LBD = Lewy Body disease; Aβ = amyloid-beta; α-syn = α-synuclein; IHC = immunohistochemistry.

Figure 2 Differences in MRI volume between LATE-NC and non-LATE-NC donors. Figure **A** shows the difference in amygdala and hippocampal volume (in mm^3) between LATE-NC and non-LATE-NC donors. Figure **B** shows the difference in amygdala and hippocampal volume between LATE-NC AD and non-LATE-NC AD donors. Figure **C** shows the difference in

amygdala and hippocampal volume between LATE-NC LBD and non-LATE-NC LBD donors. *p<0.05; **p<0.01.

Figure 3 Amygdala and hippocampal subregion volumes Differences in amygdala subnuclei (**A**) and hippocampal (**B**) subfield volumes in LATE-NC and non-LATE-NC donors. *p<0.05; **p<0.01.

Figure 4 Area under the curve for MTA score, amygdalar, and hippocampal volumes. The area under the curve (AUC) distinguishing LATE-NC from non-LATE-NC donors is similar for MTA score (.716), (ICV corrected) amygdalar (.777) and hippocampal (.715) volumes.

Figure 5 *in-vivo* MRI volumes. Figure **A** shows differences in *in-vivo* amygdala and hippocampal volumes between LATE-NC and non-LATE-NC AD donors. Figure **B** shows the correlation between post-mortem and *in-vivo* MRI, corrected for amount of time between the two scans.

Figure 6 differences in pathological load between LATE-NC and non-LATE-NC donors. Figure A shows the difference in TDP-43 density (**A, B**) amyloid-β load (**C, D**) and p-tau load (**E, F**) in LATE-NC and non-LATE-NC donors. *p<0.05; **p<0.01.

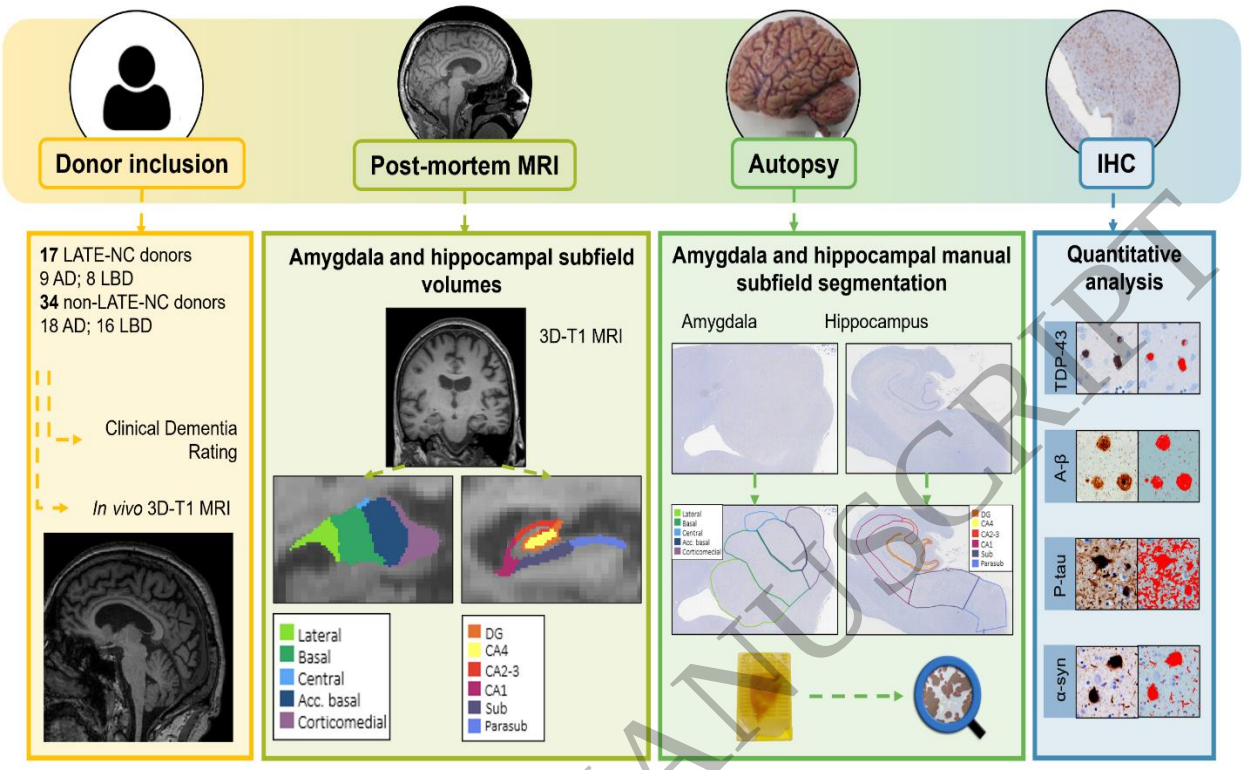

Figure 1
311x167 mm (x DPI)

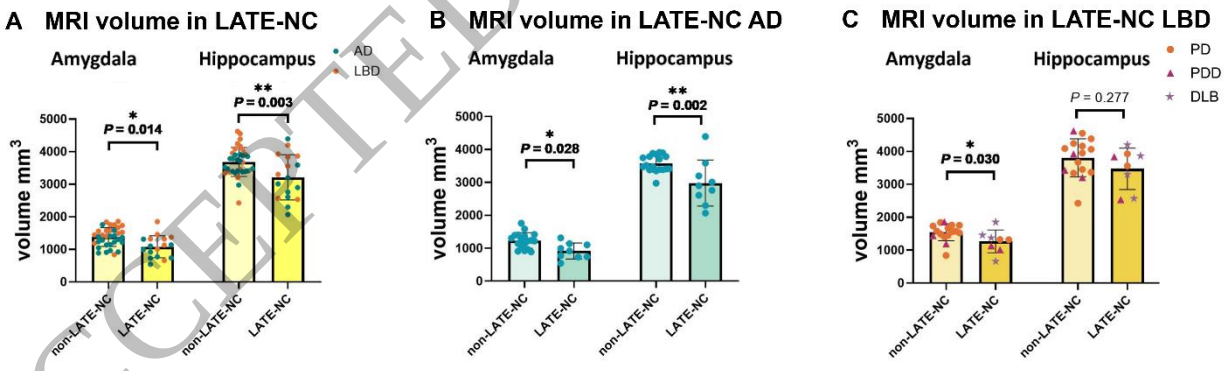

Figure 2
331x98 mm (x DPI)

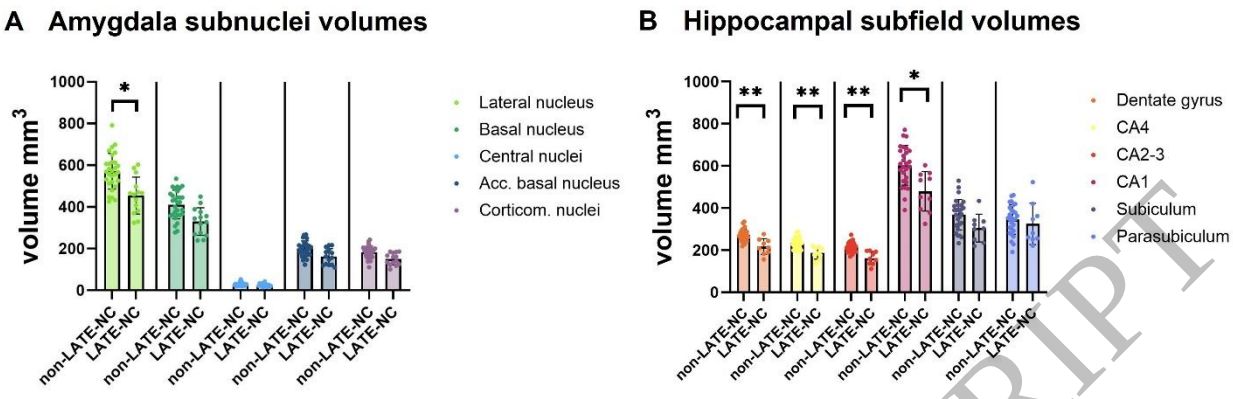

Figure 3
328x106 mm (x DPI)

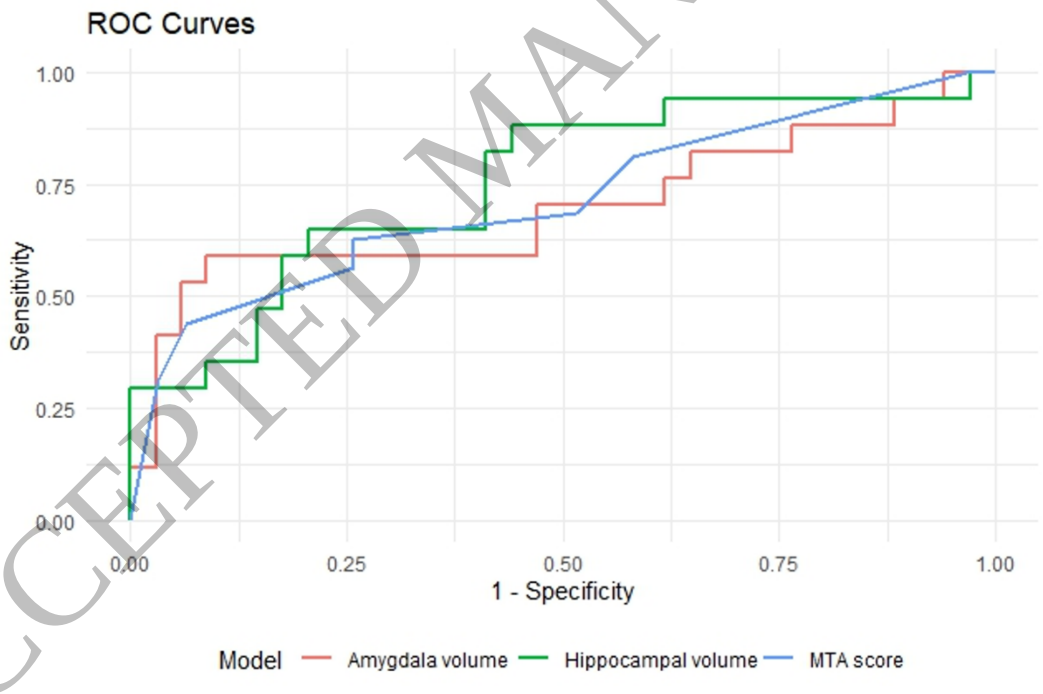

Figure 4
166x110 mm (x DPI)

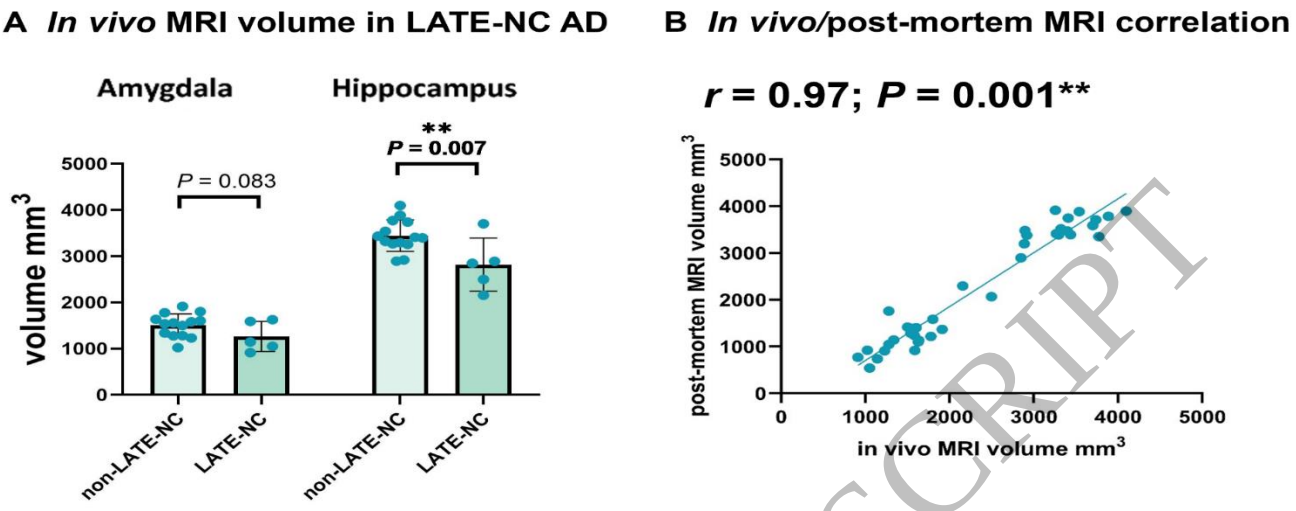

Figure 5
220x105 mm (x DPI)

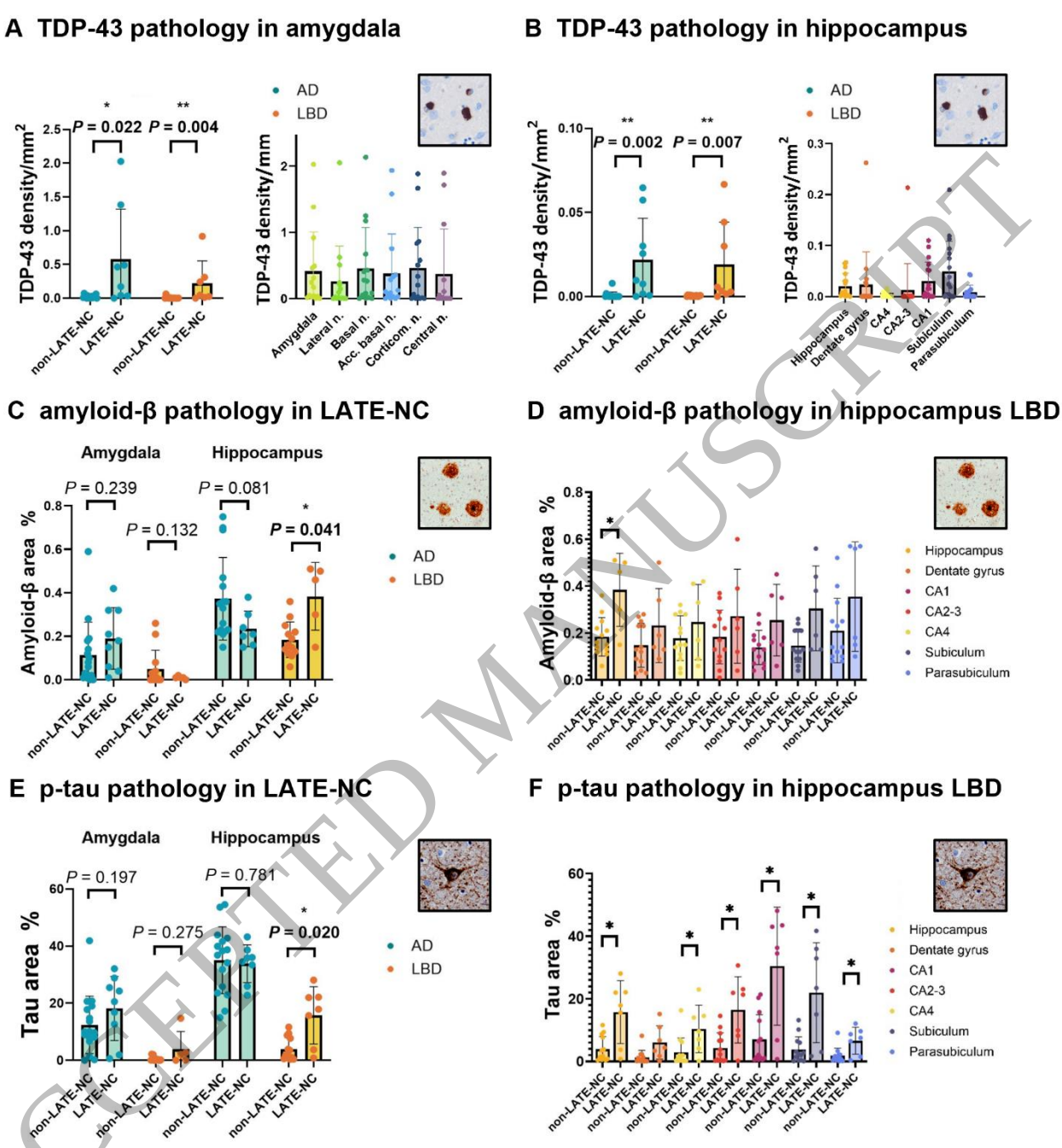

Figure 6
168x179 mm (x DPI)

TYSABRI™ (natalizumab)
SUBCUTANEOUS USE | 300mg

Prescribing Information

Efficacy made Convenient

TYSABRI SC injection with the potential to administer **AT HOME** for eligible patients*

Efficacy and safety profile comparable between TYSABRI IV and SC†[1,2]

†Comparable PK, PD, efficacy, and safety profile of SC to IV except for injection site pain.[1,2]

CLICK HERE TO DISCOVER MORE ABOUT TYSABRI SC AND THE DIFFERENCE IT MAY MAKE TO YOUR ELIGIBLE PATIENTS

Supported by

BIOGEN'S Stratify JCV™ SERVICE

A Biogen developed and funded JCV antibody index PML risk stratification service, validated and available exclusively for patients on or considering TYSABRI.

*As of April 2024, TYSABRI SC can be administered outside a clinical setting (e.g. at home) by a HCP for patients who have tolerated at least 6 doses of TYSABRI well in a clinical setting. Please refer to section 4.2 of the SmPC.[1]

TYSABRI is indicated as single DMT in adults with highly active RRMS for the following patient groups:[1,2]

- **Patients with highly active disease despite a full and adequate course of treatment with at least one DMT**
- **Patients with rapidly evolving severe RRMS defined by 2 or more disabling relapses in one year, and with 1 or more Gd+ lesions on brain MRI or a significant increase in T2 lesion load as compared to a previous recent MRI**

Very common AEs include nasopharyngitis and urinary tract infection. Please refer to the SmPC for further safety information, including the risk of the uncommon but serious AE, PML.[1,2]

Abbreviations: AE: Adverse Event; **DMT:** Disease-Modifying Therapy; **Gd+:** Gadolinium-Enhancing; **HCP:** Healthcare Professional; **IV:** Intravenous; **JCV:** John Cunningham Virus; **MRI:** Magnetic Resonance Imaging; **PD:** Pharmacodynamic; **PK:** Pharmacokinetic; **PML:** Progressive Multifocal Leukoencephalopathy; **RRMS:** Relapsing-Remitting Multiple Sclerosis; **SC:** Subcutaneous.

References: 1. TYSABRI SC (natalizumab) Summary of Product Characteristics. **2.** TYSABRI IV (natalizumab) Summary of Product Characteristics.

Adverse events should be reported. For Ireland, reporting forms and information can be found at www.hpra.ie. For the UK, reporting forms and information can be found at https://yellowcard.mhra.gov.uk/ or via the Yellow Card app available from the Apple App Store or Google Play Store. Adverse events should also be reported to Biogen Idec on MedInfoUKI@biogen.com 1800 812 719 in Ireland and 0800 008 7401 in the UK.

Biogen-261128. DOP: April 2025

Biogen